LASER COMPTON SCATTERING X-RAYS AS A TOOL FOR K-EDGE DENSITOMETRY*

M. Titberidze†, Physics Department, Idaho State University, Pocatello, ID 83209, USA
K. Chouffani, Idaho Accelerator Center, Pocatello, ID 83209, USA

Abstract

There is a huge interest in bright and tunable X-ray sources. These sources can be used in various research fields, including medical, biological and industrial fields. Laser Compton Scattering (LCS) technique gives us possibility to generate tunable, quasi monochromatic and polarized X-ray beam [1, 2]. One of the applications of LCS is the detection and quantitative identification of special nuclear materials (SNM) using K-edge densitometry (KED) method. Our group was the first one who has used a quasi-monochromatic LCS source to carry out KED experiments. The experiments showed that LCS technique could be used for SNM detection and quantification.

INTRODUCTION

A non destructive technique also known as non destructive assay (NDA) is very important for nuclear non-proliferation. Hybrid K-edge densitometry (HKED) has been widely used around the world for identification and quantification of SNM [3]. Using KED technique the density of an analyte can be determined selectively from transmission measurements below and above the absorption edge of an analyte. This technique was introduced and developed by H.Ottmar *et.al.* [4] who have pioneered in HKED technique using X-rays from conventional X-ray tubes. At Los Alamos National Laboratory the group of Nuclear Non-Proliferation and Safeguards is still actively using X-ray tube based Hybrid K-edge Densitometer to identify and quantify SNM in liquid solutions. For the same application as described earlier (KED), our group at the Idaho Accelerator Center (IAC) used LCS X-rays over X-rays from conventional X-ray tubes because of following main reasons:

- The ability to tune the photon energy to the absorption edge of SNM.
- The quasi-monochromatic feature, which yields high signal to noise ratio, while X-ray tubes generate unnecessary photons, which contribute mainly to the background [4].

In this paper, we describe the theory and experiment of LCS process for 180° scattering geometry, we show the spectroscopy of LCS photons and data analysis of recorded spectra for KED. Finally, we present the measured KED experimental results using LCS.

* Work supported by DOE Grant # DE-FG07-08ID14924
† titbmikh@isu.edu

THEORY OF LCS

The head on head collision of a laser beam with a relativistic electron beam generates backscattered photons, because of the Compton Scattering. It is the same type of radiation mechanism as undulator or channeling radiations [5, 6].

Kinematics of LCS

The schematic illustration of the scattering process for 180° geometry can be found in [8] and [13].

From the energy-momentum conservation in the laboratory frame, the backscattered photon energy can be written as following [1, 2], [7, 8].

$$E_\gamma = \frac{(1+\beta)E_L}{1-\beta\cos\theta + (\frac{E_L}{mc^2})\gamma^{-1}(1+\cos\theta)}. \quad (1)$$

Here, E_γ and E_L are scattered and incident photon energies respectively, β and mc^2 are electron's velocity and rest energy. θ is a scattering angle, while γ is a relativistic Lorentz factor. Eq. (1) can be further simplified. Assuming, that the incident electrons are highly relativistic $\beta \to 1$ and scattering angle is very small $\theta \to 0$, we can rewrite Eq. (1) as following:

$$E_\gamma = \frac{4\gamma^2 E_L}{1+(\frac{4\gamma E_L}{mc^2})+\gamma^2\theta^2} \quad (2)$$

Therefore, the maximum backscattered photon energy is twice doppler upshifted laser photon energy. $E_\gamma^{max} = 4\gamma^2 E_L$.

Differential Cross Section of LCS

The differential cross section of LCS can be derived from the classical definition of the differential cross section discussed by J.D. Jackson [9]. The differential cross section of Compton scattering in electron's rest frame, first was derived by Klein and Nishina and is called Klein-Nishina formula [10], which is given by,

$$\left(\frac{d\sigma}{d\Omega}\right)_{er} = r_0^2 R^2 \left(|\vec{\epsilon}' \cdot \vec{\epsilon}|^2 + \left(\frac{R}{4} + \frac{1}{4R} - \frac{1}{2}\right)\right), \quad (3)$$

where, $r_0 = \frac{e^2}{mc^2} = 2.82 \times 10^{-13}$ cm is classical electron radius, ϵ and ϵ' are the incident and scattered photon polarization vectors respectively. R is a ration of incident to scattered wave numbers of the electromagnetic radiation.

In order to calculate differential cross section in laboratory frame we need to perform Lorentz transformations of

Eq. (3). Hence, the differential cross section of LCS for a given scattering geometry can be written as:

$$\frac{d\sigma}{d\Omega} = r_0^2 \left(\frac{1-\beta^2}{(1-\beta\cos\theta)^2} \right) \times \left(\frac{1+\cos 2\phi}{2} \left(\left(\frac{\cos\theta - \beta}{1-\beta\cos\theta} \right)^2 - 1 \right) + 1 \right), \quad (4)$$

where, $d\Omega = \sin\theta d\theta d\phi$ is a unit solid angle. θ and ϕ are the scattering and azimuthal angles respectively. Eq. (4) was derived for a linearly polarized laser beam.

LCS Energy Spectrum

LCS energy spectrum can be derived from Eq. (4). The number of scattered photons per unit solid angle per second can be written as [11]:

$$\frac{dN}{d\Omega} = L\frac{d\sigma}{d\Omega}(E,\Omega). \quad (5)$$

Here, N represents number of scattered photons, while L is the luminosity. The luminosity of LCS type of radiations was derived by Blumberg *et.al.* [1, 2, 12] and can be written as:

$$L = \frac{N_e N_L}{A} f, \quad (6)$$

where, N_e and N_L are number of electrons and number of laser photons per bunch respectively. f is a number of collisions per second. A is an effective overlap area of interaction and can be derived as following [12]. $A = 2\pi\sqrt{\sigma_L^2 + \sigma_{ex}^2}\sqrt{\sigma_L^2 + \sigma_{ey}^2}$. σ_L is a root mean square (rms) value of laser beam radius and σ_{ex} and σ_{ey} are rms width and rms height of electron beam. For the equation A, we made an assumption that laser beam is a so called pencil beam (no divergence) and electron beam has a Gaussian profile horizontally and vertically.
Assuming that, the electron beam energy and angular spreads follow Gaussian distribution, we obtain following expression for energy spectrum of LCS [1, 2].

$$\frac{dN_\gamma}{dE_\gamma} \propto L \int_0^\infty \int_0^{2\pi} \frac{d\sigma}{d\Omega} d\Omega_{det} \exp\left(-\frac{(E-E_0)^2}{2\sigma_e^2} \right) \times \exp\left(-\frac{(\theta_{x,d}-\theta_x)^2}{2\sigma_x^2} \right) \exp\left(-\frac{(\theta_{y,d}-\theta_y)^2}{2\sigma_y^2} \right) dE d\phi. \quad (7)$$

Here, $\frac{d\sigma}{d\Omega}$ is given by Eq. (4). θ, ϕ and θ_d, ϕ_d are scattered photon and detector angles respectively. $\theta_{x,d} \approx \theta_d \cos\phi_d$, $\theta_{y,d} \approx \theta_d \sin\phi_d$, while $\theta_x \approx \theta\cos\phi$, $\theta_y \approx \theta\sin\phi$, $d\Omega_{det} = d\theta_{x,d} d\theta_{y,d}$ is a solid angle subtended by the detector.

EXPERIMENTAL RESULTS AND DISCUSSIONS

Electron Linear Accelerator (LINAC)

Relativistic electrons were generated from the 44 MeV normal conducting L-band LINAC at the Idaho Accelerator Center(IAC). The layout of the LINAC can be found in [7]. The typical bunch charge was about one third of a nC and bunch length was approximately order of 100 ps.

Laser

Custom built 4 GW peak power, Nd:YAG laser was used for LCS experiments. For this experimental purposes we selected 266 nm wavelength, the fourth harmonic of fundamental wavelength, with pulse length of 270 ps. The repetition rate of laser and electron beam was set to 60 Hz.

LCS spectroscopy

In order to record the LCS spectrum, we used high purity germanium detectors (HPGe). The recorded spectra including spectral pile-ups due to detector resolving time are shown on Fig. 1 and Fig. 2.

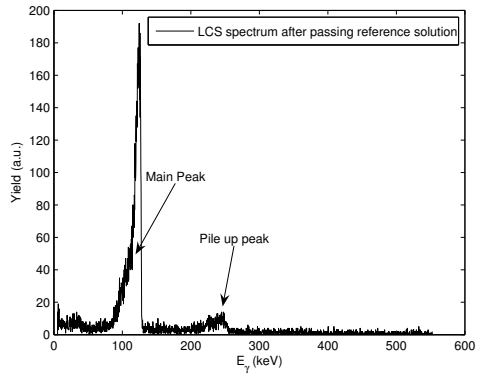

Figure 1: LCS spectrum recorded by HPGe detector, after passing nitric acid reference solution.

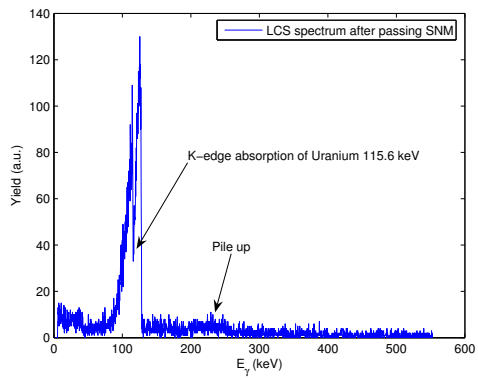

Figure 2: LCS spectrum recorded by HPGe detector, after passing uranium solution.

As we can see from Fig. 1, the recorded spectrum of LCS X-rays is in a good agreement with the theoretically predicted spectrum (see [1, 2]). The peak energy of the LCS spectrum is around 125 keV. The K-shell electron binding energy is 115.6 keV. Therefore, one can notice in Fig. 2 that, there is an absorption in the main peak around 116 keV due to the photo electric effect. Basically, the depth of the absorption in the peak is a measure of how much uranium is in the sample.

KED Analysis

To analyze the recorded spectra of LCS for KED purposes we adapted the same technique used by H.Ottmar [4], where the density of SNM is defined as following [4].

$$\rho(g/L) = \frac{\ln\left(\frac{T(E_-)}{T(E_+)}\right)}{\Delta\mu \cdot d} \cdot 1000 \qquad (8)$$

Where, $T(E_-)$ and $T(E_+)$ are photon transmissions below and above the absorption edge of actinide material. d is the thickness of the sample, $\Delta\mu$ is a difference of mass attenuation coefficients below and above absorption edge windows.

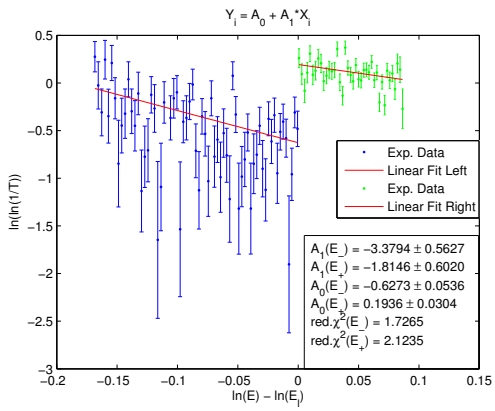

Figure 3: Linearized LCS data and fits below and above K-absorption edge, for uranium sample #1.

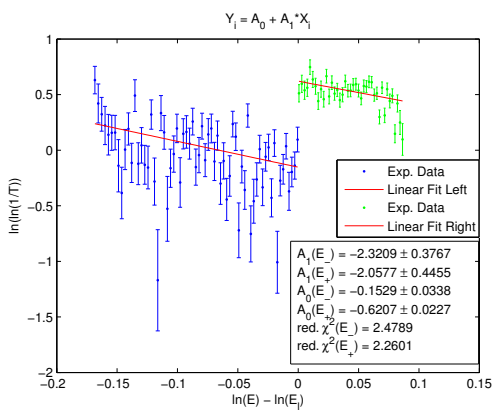

Figure 4: Linearized LCS data and fits below and above K-absorption edge, for uranium sample #2.

Results

Uranium samples dissolved in HNO_3 solution, were provided by Sandia National Laboratories. The thickness of each cuvette was $d = 2$ cm. After linearizing LCS spectra we were able to perform linear fits below and above the absorption edge. We used the fitted parameters to calculate the density of SNM. The fitted parameters and calculated densities are summarized in Tables (1) and (2).

Table 1: Final Results for Uranium Sample #1

Quantity	Below edge	Above edge	ρ (g/L)
A_0	-0.63 $\pm$ 0.05	0.19 $\pm$ 0.03	103 $\pm$ 7
A_1	-3.38 $\pm$ 0.56	-1.82 $\pm$ 0.60	
χ^2_ν	1.73	2.12	

Table 2: Final Results for Uranium Sample #2

Quantity	Below edge	Above edge	ρ (g/L)
A_0	-0.15 $\pm$ 0.03	0.62 $\pm$ 0.02	152 $\pm$ 8
A_1	-2.32 $\pm$ 0.38	-2.06 $\pm$ 0.45	
χ^2_ν	2.48	2.26	

ACKNOWLEDGMENT

I would like to thank my advisor Dr. Khalid Chouffani for his enormous work and support during this project.

REFERENCES

[1] K. Chouffani et al., Phys. Rev. ST Accel. Beams **9**, 050701 (2006).

[2] K. Chouffani et al. Laser and Particle Beams **24**, 411 (2006).

[3] D. Reilly, N.Ensslh, H. Smith, Jr., S. Kreiner. *NRC Passive Nondestructive Assay of Nuclear Materials*, March (1991).

[4] H. Ottmar, H. Eberle The Hybrid K-edge/K- XRF Densitometer: Principles-Design-Performance, February (1991).

[5] K. Chouffani and H. Überall, Theory of Low Energy Channeling Radiation: Application to a Germanium Crystal, Phys. Stat. Sol. (b) 1999, 213, No. 1, 107-151.

[6] K. Chouffani and H. Überall, Low Energy Channeling Radiation experiments in a Germanium Crystal, Nucl. Instr. And Meth. Phys. Research B **152**, 4 (1999) pp. 479-493.

[7] K. Chouffani et al. Nucl. Instr. and Meth. A **495**, 95 (2002).

[8] J. Stepanek et al. Nucl. Instr. and Meth. A **412**, 95 (1998).

[9] J.D. Jackson *Classical Electrodynamics* 3rd ed. John, Wiley and Sons, (1998).

[10] O. Klein, Y. Nishina Über die Streuung von Strahlung durch freie Elektronen nach der neuen relativistischen Quantendynamik von Dirac. Z. F. Phys. **52** (11-12) (1929).

[11] W.R. Leo *Techniques for Nuclear and Particle Physics Experiments*, 3rd ed. Springer-Verlag (1987).

[12] L.N. Blumberg Kinemarics of Compton Backscattering X-ray Source for Angiography. Brookhaven National Laboratory Report, May (1992).

[13] M. Titberidze, Master Thesis, Idaho State University, (2011).